ELSEVIER

Contents lists available at ScienceDirect

BBA - Proteins and Proteomics

journal homepage: www.elsevier.com/locate/bbapap



different

Assembly of Hydrophobin class I from *Agaricus bisporus* produced different amyloid-like fibrils

Jesús Rojas-Osnaya, Hugo Nájera

Universidad Autónoma Metropolitana-Cuajimalpa. Departamento de Ciencias Naturales. Laboratorio de Biofisicoquímica, Av. Vasco de Quiroga 4871. Col. Santa Fe Cuajimalpa, Alcaldía Cuajimalpa, Mexico City, CP 05348, Mexico

ARTICLE INFO

Keywords: Agaricus bisporus Hydrophobin Surface activity Fibrillogenesis

ABSTRACT

This work studied the extraction, purification, characterization, and assembly of hydrophobin class I from *Agaricus bisporus* (ABH4). The highest soluble protein concentration was obtained from the pinhead, the extraction and purification were efficient for hydrophobin class I, obtaining a band of 12 kDa. The identified sequence of hydrophobin presented the eight cysteine residues; for the prediction of the structure, hydrophobin presented more alpha helix structures than beta sheets. It was observed that the hydrophobin managed to decrease and increase the contact angle in Teflon and glass, respectively, finding a micellar critical concentration of 221 μ g mL⁻¹. ThT experiments demonstrated that the production of fibrils decreased at basic pH, while acidic and neutral pH favoured the formation of fibrils. Likewise, the addition of colloidal Teflon affects the formation of fibrils. Circular dichroism spectra proved that hydrophobin class I undergo changes in its secondary structure, increasing its alpha helix and beta sheet content after vortexing. It was observed that the analysis by scanning electron microscopy and atomic force microscopy of the hydrophobin produced different amyloid-like structures in glass and mica.

1. Introduction

Fungi are essential organisms in nature; some contain beneficial effects while others are pathogenic. Many species have long been used in traditional medicines or functional foods in many countries. There is great interest in the secondary metabolites of fungi due to many applications [1,2]. Among the macroscopic fungi is Agaricus bisporus, a mushroom that contains a wide variety of compounds, and proteins beneficial to humans. Several compounds have been isolated, including pigments, polysaccharides and proteins such as lectins, tyrosinases and hydrophobins [3,4]. Hydrophobins (Hfb) are small extracellular proteins produced by fungi. They contain between 100 and 150 amino acids and have a conserved domain of eight cysteine residues. They are classified according to their solubility and ability to form stable structures called rodlets, which are amyloid-like. Hydrophobins class I (Hfb-I): can be dissolved with trifluoroacetic acid (TFA) or formic acid and can form rodlets; hydrophobins class II (Hfb-II): are soluble in 2 % sodium dodecyl sulfate (SDS) or 60 % ethanol, they are not capable of forming rodlets [5]. Hfb also perform different functions, including breaking down the water layer by lowering surface tension for hyphal growth, binding to hydrophobic substrates, and coating spores and fruiting bodies [4]. Likewise, they been reported to participate in the symbiotic association of fungi and plants or algae and/or cyanobacteria [6]. The amphipathic nature of Hfb is essential to change the nature of the surface from hydrophilic to hydrophobic or vice versa; at the water-air interface, Hfb-I produce surface films in the form of mono-multilayers, while Hfb-II are monolayers [7,8]. Hydrophobins are related to the formation of amyloid-type structures on hydrophilic and hydrophobic surfaces, which entails many benefits, such as a decrease in surface tension and protecting parts of fungi against wetting and desiccation [9]. Conformational changes accompany the self-assembly of Hfb; for the water-air interface, both Hfb are rich in β -sheet structure, while at the interface between water and hydrophobic solid, the α -helix structure increases [10,11]. This work aimed to purify and assemble the hydrophobin class I from A. bisporus (ABH4), producing different amyloid-like fibrils.

2. Materials and methods

2.1. ABH4 extraction

Agaricus bisporus (Monte Blanco, Mexico) was purchased in a local market; the pinhead, outer stipe layer, and inner stipe were washed, cut,

E-mail addresses: jrojas@cua.uam.mx (J. Rojas-Osnaya), hnajera@cua.uam.mx (H. Nájera).

https://doi.org/10.1016/j.bbapap.2024.141048

Received 30 May 2024; Received in revised form 3 September 2024; Accepted 24 September 2024 Available online 26 September 2024

^{*} Corresponding author.

and frozen at $-80\,^{\circ}$ C. Subsequently, they were fragmented separately in a blender, using a 0.1 M sodium phosphate buffer solution with 1 % SDS at pH 7 and 100 °C. The material was centrifuged at 10,000 rpm for 10 min at 4 °C, the precipitate was washed with deionized water until SDS was eliminated, and then it was lyophilized and stored at 4 °C. Freezedried pinhead, outer stipe layer and inner stipe were treated with trifluoroacetic acid (TFA) and kept stirring for 4 h at 4 °C, then centrifuged at 8000 rpm for 10 min at 4 °C. To the supernatant was added 5 mL of 60 % ethanol, and an airflow was placed using a fish tank pump overnight to remove TFA. It was centrifuged at 8000 rpm for 10 min at 4 °C to remove undissolved material, and the supernatant was lyophilized and stored at 4 °C [12].

2.2. ABH4 purification and protein content

The freeze-dried pinhead was solubilized in deionized water and adjusted to pH 7 by adding 0.1 M NaOH, then was loaded into a molecular size exclusion column (SEC) Superdex $^{\rm TM}$ 200 16/600 (GE Healthcare) and elution was carried out under an isocratic flow of 1 mL min $^{-1}$ using 0.1 M sodium phosphate buffer with added 0.15 M NaCl at pH 7, fraction collected was 1 mL, the chromatography was performed in a FPLC (ÄKTA Purifier 100, GE Healthcare). Fractions with ABH4 were subjected to an exchange to deionized water and adjusted to pH 7 using a 10 kDa membrane (Amicon, Dublin, Ireland). Soluble protein quantification was measured at 280 nm; the experiments were carried out in triplicate [13,14].

2.3. Polyacrylamide gel electrophoresis under denaturing conditions

Fractions obtained by SEC were subjected to acrylamide gel electrophoresis analysis under denaturing conditions (SDS-PAGE). 0.575 μg of protein was injected into each lane of the gel. Wide-range molecular mass standards were used as reference. The gels were stained with a Silver Stain Kit (Bio-Rad) and analyzed with ImageJ 1.52 [15].

2.4. Identification and prediction of the structure of ABH4

The purified ABH4 was analyzed by SDS-PAGE and stained with Coomassie blue R-250. The band was cut with a sterile scalpel and treated according to the following methodology. Reduced with Dithiothreitol, alkylated with Iodoacetamide, and digested "in gel" with Trypsin. A solution of 50 mM ammonium bicarbonate pH 8.2 was used in the digestion and incubated for 18 h at 37 °C. The resulting peptides were desalted with Zip-Tips with 0.6 µL of C18 resin (ZTC18S096 -Merck Millipore). Samples were analyzed by Liquid Chromatography with tandem mass spectrometry (LC-MS/MS) (Orbitrap velos-Ultimate Dionex 3000, Thermo Scientific), and results were displayed in Scaffold 5 (Proteome Software, USA). For the prediction of the structure, the ABH4 sequence was used in the Swiss Model and AlphaFold programs; for the electrostatic surface the ChimeraX 1.7.1 program was used. The sequences of Agaricus bisporus hydrophobins (ABH1, ABH2, ABH3, and ABH4) were aligned using the online program Clustal Omega, removing the signal peptide from the four hydrophobins.

2.5. Determination of the surface activity of ABH4 by contact angle measurements

The contact angle θ (°) of a drop of deionized water (1 μ L) was measured on a hydrophobic (Teflon) and a hydrophilic (glass) surface previously coated with ABH4 (7–785 μ g mL $^{-1}$), which were left dry for 12 h. Protein concentration was determined at 280 nm [13,14]; the experiments were carried out in triplicate. Contact angle measurements were conducted quadruplicated, and images were analyzed with the ImageJ 1.52 program to determine the contact angle [15].

2.6. Determination of surface tension and critical micellar concentration

The pendant drop method determined the surface tension (ST) of ABH4 aqueous solutions (7–785 $\mu g\ mL^{-1}$). Protein concentration was determined at 280 nm [13,14]; the experiments were carried out in triplicate. Images and symmetry of the pendant drop were analyzed with ImageJ 1.52. The measurements were conducted in triplicate and analyzed through the Young-Laplace model (Eq. 1) to determine the ST [16]. Critical micellar concentration was calculated using the ST values of a protein concentration curve.

$$\gamma = \frac{\Delta \rho g D^2}{H} \tag{1}$$

Where γ shows the surface or interfacial tension $[\mathbb{N} \cdot \mathbb{m}^{-1}]$, Δp is the density difference between the water and air interface, g is the gravity acceleration, D is the largest diameter in the drop, and H is the dimensionless number.

2.7. Fluorescence spectroscopy

ABH4 (108 μg mL $^{-1}$) was incubated with Thioflavin-T (ThT) in deionized water, pH 2, 5, 7, 9, 10, and 37 °C; in another experiment, it was added 0.6 % of colloidal Teflon and pH 7. ABH4 was preassembled by vortexing for 2 min. Fluorescence was determined every 5 min for 240 min, using an excitation wavelength of 450 nm and an emission wavelength of 490 nm in a spectrofluorometer ChronosBH (Illinois, USA). ThT was prepared at 10 mM in absolute ethanol; the final ThT concentration was 66 μ M.

2.8. Circular dichroism spectroscopy (CD)

ABH4 (108 µg mL $^{-1}$) was previously vortexing for 2 min and incubated at 37 °C, pH 7 for 240 min; measurements were taken every 15 min. 2 µL of concentrated TFA (99.0 %) was added to obtain the monomeric, and the final concentration of TFA was 66 %. CD spectra were obtained using a Jasco J-815 spectropolarimeter (Tokyo, Japan) equipped with a cell holder, with a Peltier temperature control and a wavelength of 250 to 190 nm, using a 0.1 cm pathlength cell; each spectrum reported is the average of 3 consecutive scans.

2.9. Scanning electron microscopy (SEM)

ABH4 ($108 \,\mu g \,mL^{-1}$) were vortexing for 2 min and incubated at 37 °C for 240 min 15 $\,\mu L$ of this solution was deposited on a cover glass and mica. Samples were dried at 37 °C for 12 h and analyzed in a scanning electron microscope Hitachi TM3030 Plus (Tokyo, Japan).

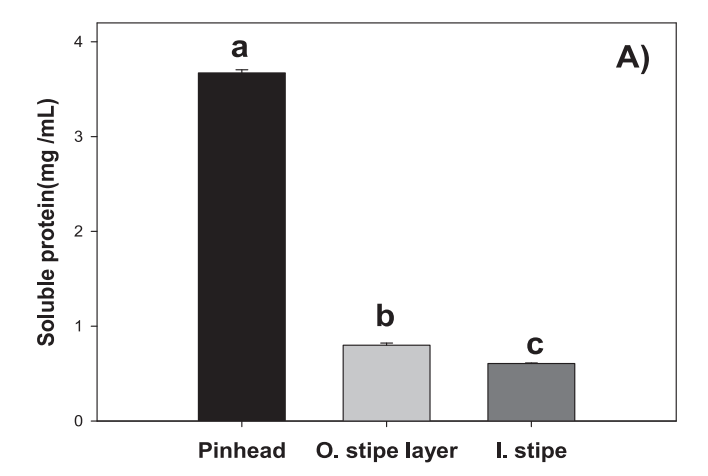
2.10. Atomic force microscopy (AFM)

ABH4 (108 $\mu g\ mL^{-1})$ was vortexed for 2 min and incubated at 37 $^{\circ}C$ for 240 min, 15 μL of this solution was deposited on a cover glass and mica. Samples were dried at 37 $^{\circ}C$ for 12 h and analyzed in a Nanosurf NaioAFM (Liestal. Switzerland), using a cantilever (ContAl-G). The images were analyzed with the Gwyddion 2.65 program to provide topography information and morphology of the surfaces formed by amyloid-like fibers.

3. Results and discussion

3.1. Extraction and purification of ABH4

The extraction and purification of ABH4 involved the collection of soluble proteins from the pinhead, outer stipe layer, and inner stipe of *A. bisporus*, as illustrated in Fig. 1A. Our analysis revealed a significantly higher concentration in the pinhead. This finding was further validated by statistical analysis. This observation is consistent with the findings of



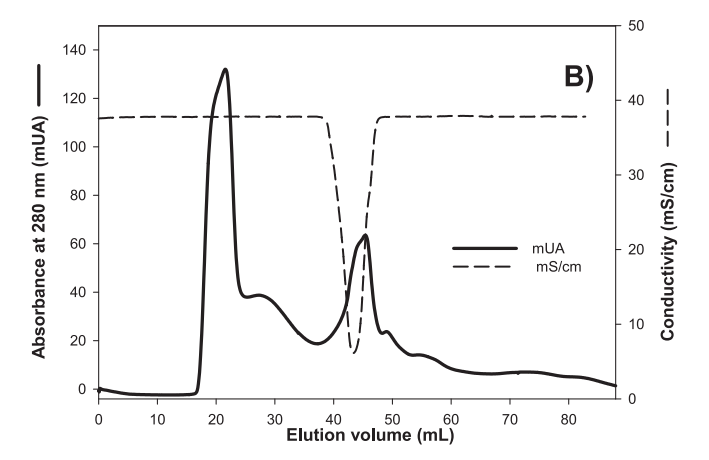


Fig. 1. (A) Soluble protein content in the pinhead, outer, and inner stipe layer. Different letters indicate significance (p<0.05) using Tukey's multiple comparison test of means. (B) Fractionation of the pinhead proteins by SEC using 0.1 M sodium phosphate buffer added with 0.15 M NaCl and pH 7.

Lugones et al. who also reported a higher concentration of soluble protein in the pinhead [12]. This could be due to other proteins and enzymes on the outer surface of the fruiting bodies serving specific functions in the mushroom. Pothiratana et al. also found a higher concentration of soluble protein in the fruiting bodies of the mushroom *Agrocybe cylindracea*, due to the presence of five hydrophobins [17]. Fig. 1B displays the chromatogram obtained by SEC from the pinhead, using 0.1 M sodium phosphate buffer added with 0.15 M NaCl and pH 7.

3.2. Polyacrylamide gel electrophoresis under denaturing conditions

Fig. 2 shows the fractions obtained by SEC, analyzed by SDS-PAGE. In fractions 18–24 (Fig. 2A), they present bands of 150 kDa and between 75 and 50 kDa. According to previous reports, these molecular weights can concern other proteins present in *A. bisporus*, such as laccases (56 kDa) and polyphenol oxidases (43 kDa) [18–21]. Fractions 43–47 (Fig. 2B) present a band of 12 kDa, this molecular weight and due to the extraction conditions, this band could be attributed to a hydrophobin class I; these results are like those reported by Rafeeq et al. They stated that the molecular weight of hydrophobins is between 7 and 15 kDa [22,23]. The extraction and purification of hydrophobins from *Agaricus bisporus* have been reported, finding proteins with a molecular weight of 8.9, 16, and 19 kDa [12,24,25]. Hydrophobin from the pinhead of *A. bisporus* presented a single protein band of 12 kDa (Fig. 2C).

3.3. Identification and prediction of the structure of ABH4

Fig. 3A presents the identified sequence of ABH4, obtained through the highly reliable LC-MS/MS analysis. The sequence has eight cysteine residues (C). It has been reported that all Hfb present these eight cysteine residues in their structure, which form four disulfide bridges, generating four loops, which confer stability to the protein in its monomeric and folded form [4,26].

The identified sequence of ABH4 was aligned with the sequences of other hydrophobins present in *A. bisporus* (ABH1, ABH2, and ABH3) (Fig. 3A), which shows similarities and differences between them. The eight cysteine residues of the four hydrophobins are found in the same position within their primary structure; each cysteine residue will be found in a particular position due to the number of amino acids between each cysteine, the four hydrophobins of *A. bisporus* presented this pattern. The literature has reported that this pattern differentiates hydrophobins class I from class II. According to this, the four hydrophobins of *A. bisporus* are class I [8,27].

According to Linder and co-workers, both classes of hydrophobins (I and II) in their sequences contain eight cysteine residues in a unique particular pattern; the second and third cysteine residues are close to each other forming a pair; this also occurs in cysteine residues sixth and seventh. In this case, the cysteine residues in the ABH1, ABH2, ABH3, and ABH4 sequences present this pattern. Furthermore, this pattern allows the cysteine residues to be easily recognized in the four sequences and present symmetry. ABH4 presents sequences conserved (*) with the other hydrophobins of A. bisporus; between the amino acids at positions 52 and 96, the four hydrophobins present glycine and leucine residues. In this regard, Tyminski et al. reported that hydrophobins contain four disulfide bridges in their structure, with eight cysteine residues forming four loops in the sequence [28]. These loops have specific characteristics: the first loop usually contains 5-9 amino acid residues, and the second loop contains at least one glycine residue, which usually adheres to a hydrophobic amino acid. In the present study, the four hydrophobins from A. bisporus contain 5-9 amino acids in the first loop. Likewise, the second loop contains glycine residues close to the hydrophobic amino acids leucine and valine. Some differences in the sequence were that ABH4 has fewer proline residues, unlike ABH2 and ABH3, which presented this amino acid in their sequence, while ABH1 presents a threonine residue. Another difference is that ABH4 presented 26 amino acids in its signal peptide, while ABH1, ABH2, and ABH3 presented 19, 22, and 19, respectively. Fig. 3B shows the prediction of the structure of ABH4; it is observed that ABH4 mainly presents α helical structures and β sheets. For the electrostatic surface (Fig. 3C and D), ABH4 presents a homogeneous distribution of charges in its structure.

3.4. ABH4 surface activity by contact angle

Surface activity was studied by measuring the contact angle at different concentrations of ABH4 (Fig. 4) on Teflon (4 A) and glass (4B). Fig. 4A exhibits the contact angle values, showing a difference concerning the control (129.58 \pm 3.52), decreasing the contact angle after treatment with ABH4. For the surface activity in glass, there was also a difference to the control (17.66 \pm 1.83), increasing the contact angle; no significant differences in surface activity were found for Teflon or glass at concentrations >42 μg mL $^{-1}$. These results are similar to Lugones et al. [12], where the Teflon surface was treated with Hfb (20 μg mL $^{-1}$), obtaining a 57 % reduction in the contact angle, and Vigueras et al., where the hydrophobin from *Paecilomyces lilacinus* decreased the contact angle from 130 to 47 using 450 μg mL $^{-1}$ of the hydrophobin solution [29,30].

3.5. Surface tension and critical micellar concentration

Changes in surface tension at different concentrations of ABH4 are shown in Fig. 5; when the protein concentration increased, the surface

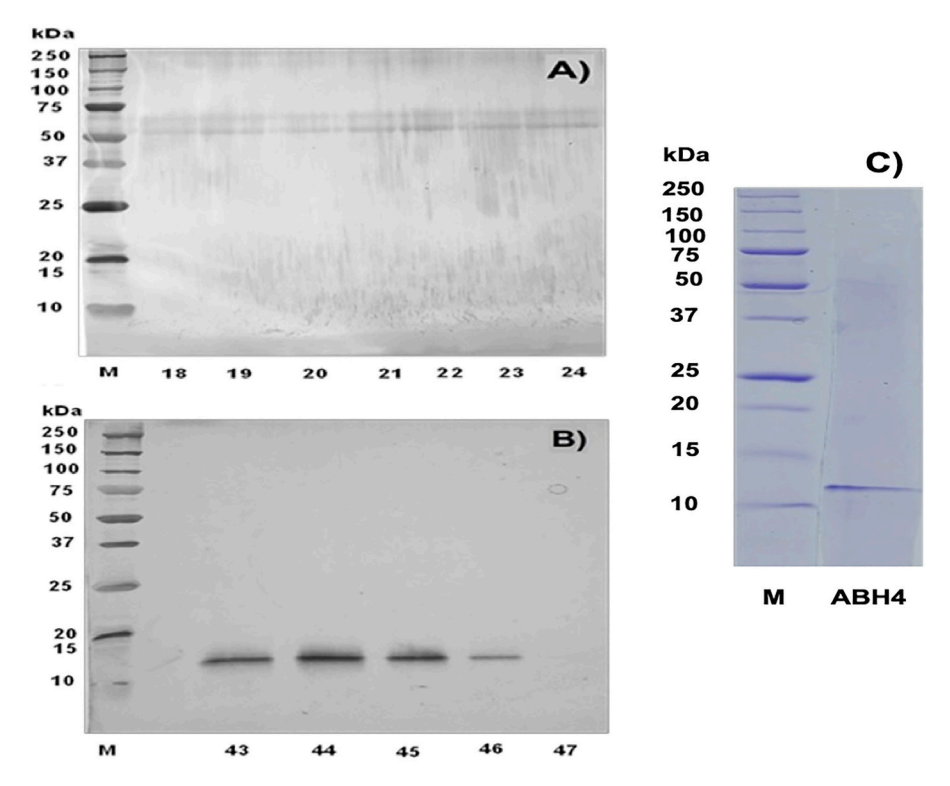


Fig. 2. SDS-PAGE of SEC fractions 18–24 (A) and 43–47 (B) using 0.1 M sodium phosphate buffer added with 0.15 M NaCl and pH 7. (C) ABH4 and molecular weight markers (M) were stained with Coomassie blue R-250. (For interpretation of the references to colour in this figure legend, the reader is referred to the web version of this article.)

tension of a drop of deionized water decreased (Fig. 5B). Interestingly, at concentrations above 200 µg mL⁻¹, no significant differences in the change of surface tension were observed. The critical micellar concentration, a critical parameter, was determined at 221 μg mL⁻¹, with a corresponding surface tension value of 38.36 mN m⁻¹. This decrease in water surface tension can be attributed to the formation of an amphipathic film by assembling the hydrophobins at the air/water interface. In previous work, Paslay et al. reported that a solution of hydrophobin (30 μg mL⁻¹) from A. bisporus (ABH1) decreased the surface tension of pure water from 74 mN m⁻¹ to 45 mN, in a short time [25]; the authors attribute this to the high protein mobility at the solution surface and produce the amphipathic film, our results indicate that ABH4 can also moves quickly to the water/air interface and assemble into a rodlet morphology, however, ABH4 needs a concentration of 71 μg mL⁻¹ to reduce the surface tension of water to 45 mN. In this regard, Kallio et al. reported that the formation of layers by hydrophobins at an oil/water or air/water interface is linked to the formation of oligomers, which arrange themselves, rendering the hydrophobic areas of the hydrophobins inaccessible to the solvent [7].

3.6. Effect of pH and colloidal Teflon concentration in fibrillogenesis of ABH4

The effect of pH on fibrillation was studied; these results are shown in Fig. 6A. The highest production of fluorescence intensity was obtained at pH 7 (ca. 2700 au) at 240 min. In contrast, the lowest was at pH 10, getting 67 % of fluorescence intensity, while when adding colloidal Teflon (6B) in concentrations of 0.4 and 0.6 %, the fluorescence intensity decreased to 54 and 57 %, respectively. This effect is less observed in concentrations of 0.2 and 1 % Teflon since the fluorescence decreased by approximately 10 and 16 % compared to pH 7. According to Biancalana and Koide, ThT is used for aggregation kinetics because it forms a specific union with amyloid fibers, causing an increase in fluorescence. Herein, the acidic and neutral pH increased the fluorescence

[31]. Contrastingly, the fluorescence intensity decreased at pH values above 9 [32]; the affinity of ThT is more significant at neutral pH than at acidic pH due to the electrostatic repulsion of the dye by an increase in positive charge. On the other hand, the sample without vortexing (WV) got 8 % fluorescence intensity at 240 min, indicating that the protein was not forming fibers. In this regard, Torkkeli et al. reported that vortexing the hydrophobin solution for 1 min helped to preassemble the proteins and start with the formation of fibers [33].

3.7. Changes in the secondary structure of ABH4 by circular dichroism

According to Wösten and de Vocht, determining secondary structure by circular dichroism of the hydrophobins class I presents a signal at 208–210 nm, indicating that proteins are rich in β-sheet structure. However, the signal may change between 215 and 217 nm due to the nature of the hydrophilic-hydrophobic interface [10]. This change can be observed when the hydrophobin solution is vortexed in the water-air interface for some time. Fig. 7 shows the results of the changes in the secondary structure of ABH4 by circular dichroism after vortexing and incubating for 240 min; as the incubation time progressed, the signal at 215 and 222 decreased, while hydrophobin without vortexing (HfbWV) and incubating at 240 min (HfbWV240 min) the signals did not modify considerably. On the other hand, the monomer of ABH4 did not present a positive increase in the signal at 195 nm, and the signal at 220 nm is not present, unlike the vortexed samples. The maximum negative increase in the signal at 220 of the vortexed samples was at 60 min of incubation, after which this signal increased positively. In addition, all spectra presented a signal around 195 nm, indicating that ABH4 also has α -helix segments in its structure. The latter is corroborated by Manavalan and Johnson [34], where the proteins α/β (intermixed segments of α -helix and β -sheet) present characteristic signals at 208 and 220 nm. Our results could indicate that ABH4 presents an intermediate with a larger α -helix structure until 60 min of incubation because the signal at 222 nm decreased, while the signal at 208 nm was maintained. After

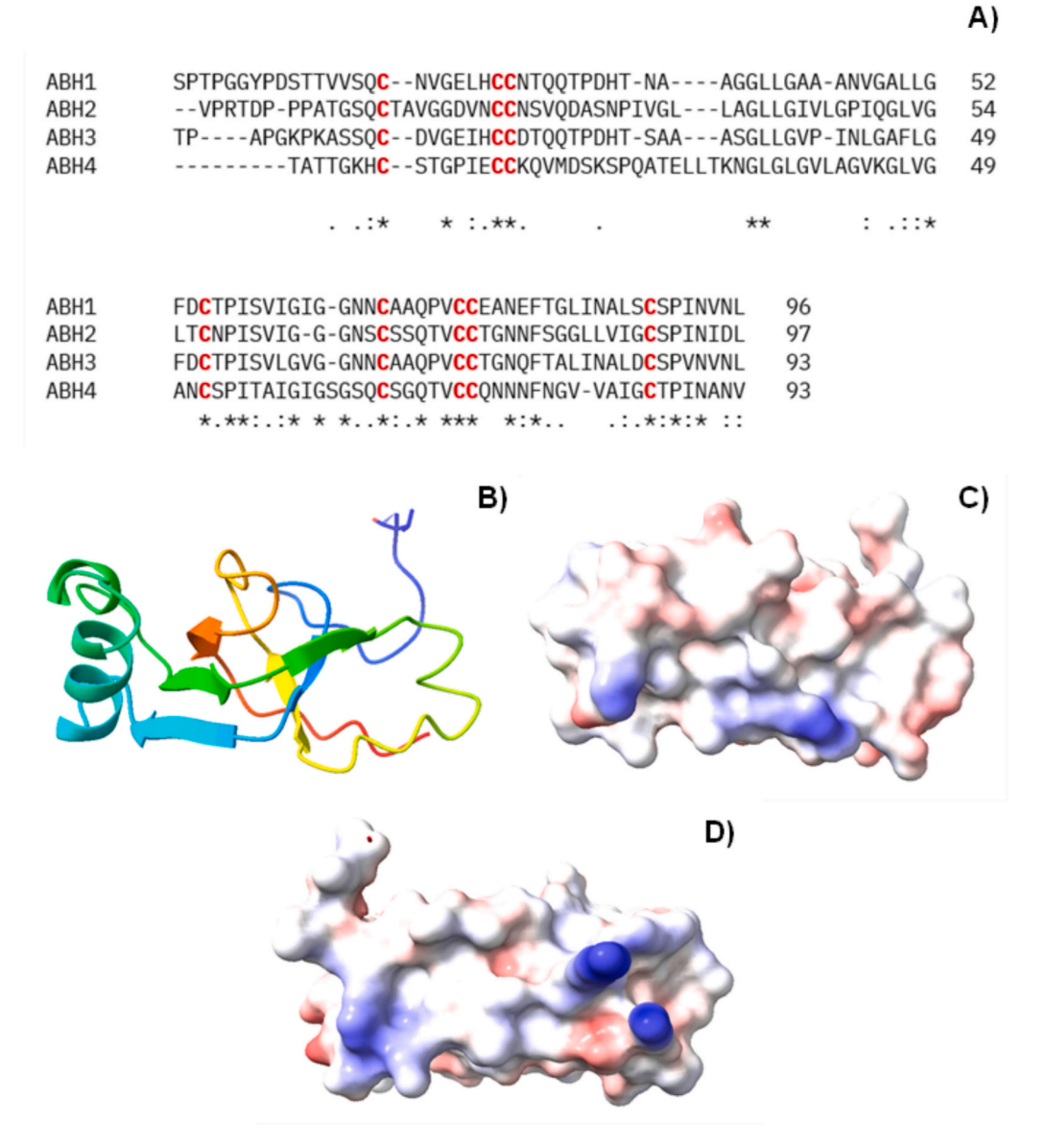


Fig. 3. Alignment of the hydrophobin sequences from A. bisporus (A), prediction of the structure of ABH4 using AlphaFold (B), and different perspectives of the electrostatic surface of ABH4 (C) and (D).

that time, the 222 nm signal increased, while the 208 nm signal decreased, suggesting that intermediary structures form during the kinetic process until they reach fibers. This result coincides with the maximum reached in the ThT experiments (ca. 60 min); after that time, the fibers mostly grow in length.

3.8. SEM and AFM measurements

Fig. 8 shows the production of large fibers on different surfaces and analyzed by SEM, finding parallel rodlets in glass (Fig. 8A) with a size of $\approx 3~\mu m$; it can also be seen that the large fibers grew in the form of branches and have a crystalline needle structure. On the other hand, the large fibers produced in mica (Fig. 8D) present a more amorphous agglomerate, indicating that the assembly of ABH4 on mica is different; this can be attributed to the fact that hydrophobins can produce different types of fibers depending on the surface on which they are found. These large fibers have very similar characteristics to amyloid fibers and can be characterized by SEM and AFM. Fig. 9 shows the production of fibers on different surfaces and analyzed by AFM, finding aligned parallel rodlets in glass (Fig. 9A) with a size of 5 μm , while in

mica, the self-assembled present amorphous agglomerate better distributed on the surface (Fig. 9C). It has been reported that morphology of amyloid-type-like fibers is indicative of self-assembled proteins rich in cross β -sheet secondary structures [17]. The results of SEM and AFM indicate that ABH4 changes its structure depending on the surface on which they are found; it adopts an amyloid-like fibers morphology in glass as it assembles, while it adopts an amorphous agglomerate in mica.

Varó and Szegletes reported that mica is a chemically inert surface, has a net negative charge with an average surface charge density $(-0.0025 \mathrm{C\ m}^{-2})$, its crystalline structure is characterized by its layered structure, along this layer, the cleavage yields an atomically flat surface; glass is also a hydrophilic surface [35]. However, it has an amorphous surface. They also reported that the lipid polar heads interact with the mica surface, thus exposing the hydrophobic tails to the environment. In the present study, ABH4 produced different types of fibers in mica and glass, suggesting that the polar part of the fibers is interacting with the mica, causing changes in the structure of the fibers. Also, mica has a flat surface, proposing that these two factors could lead to the formation of amorphous structures in mica.

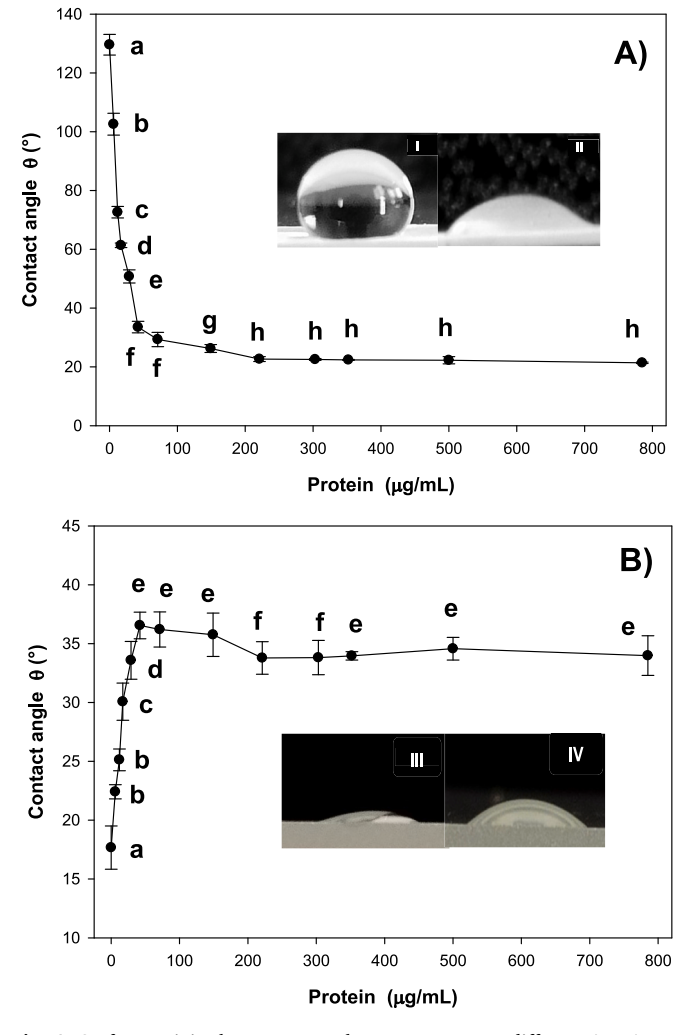


Fig. 4. Surface activity by contact angle measurement at different ABH4 concentrations on Teflon (A) and glass (B). (I) Control-Teflon, (II) ABH4-Teflon, (III) Control-glass, and (IV) ABH4-glass. Different letters indicate significance (p<0.05) using Tukey's multiple comparison test of means.

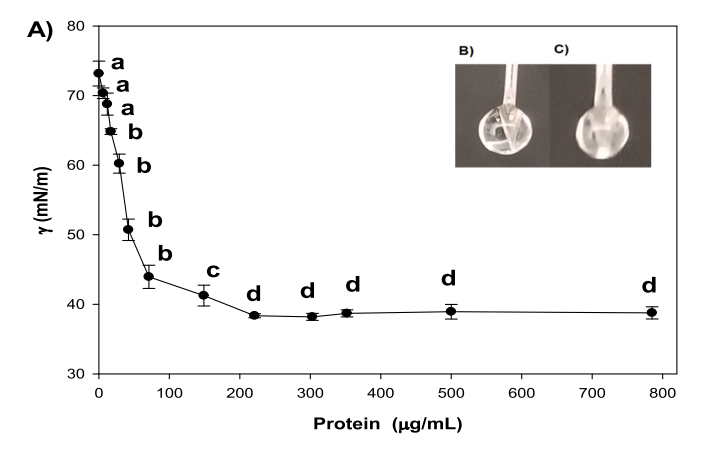


Fig. 5. Surface activity of ABH4 determined by the pendant drop method. (A) Measurements of surface tension at different protein concentrations (B) Deionized water drop and critical micelle concentration (221 μ g mL⁻¹) (C).

On the other hand, when the fibers interact with the glass surface, the hydrophilic part of the fibers would also interact with the hydrophilic part of the glass. However, the surface of the glass is amorphous; this would allow the fiber to have a different arrangement, presenting

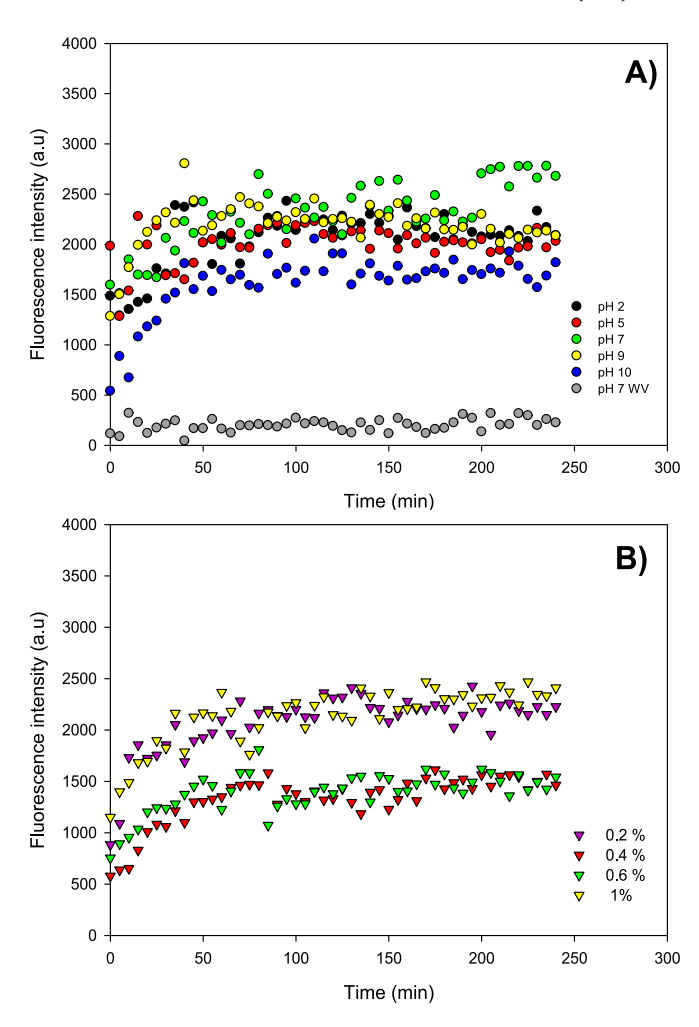


Fig. 6. Effect of pH (A) and colloidal Teflon concentration (B) in fibrillogenesis of ABH4 at 37 $^{\circ}$ C.

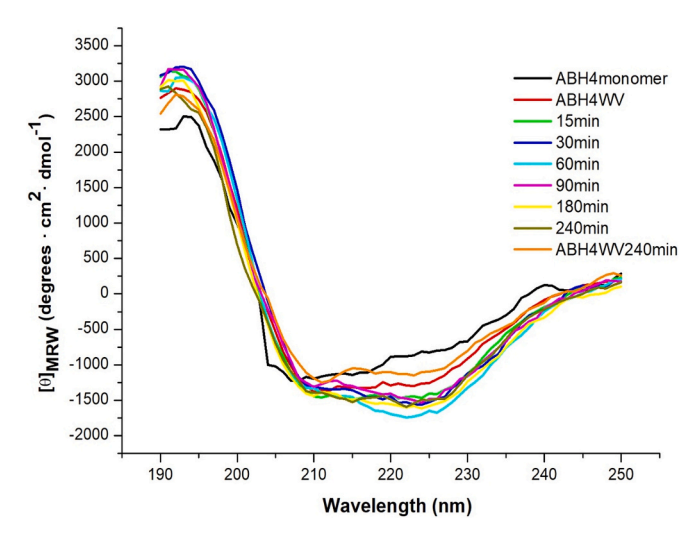


Fig. 7. CD spectra of ABH4 were determined at pH 7 and 37 $^{\circ}\text{C}$ at different times until 240 min.

aligned parallel rodlets in the glass. According to this, Cicatiello et al. reported similar results: the hydrophobins Pac2 and Pac3, from marine strains *Penicillium roseopurpureum* MUT 4892 and *Acremonium sclerotigenum* MUT 4872, Pac2 produced a compact layer formed by spherical oligomers in mica. At the same time, on a hydrophobic surface,

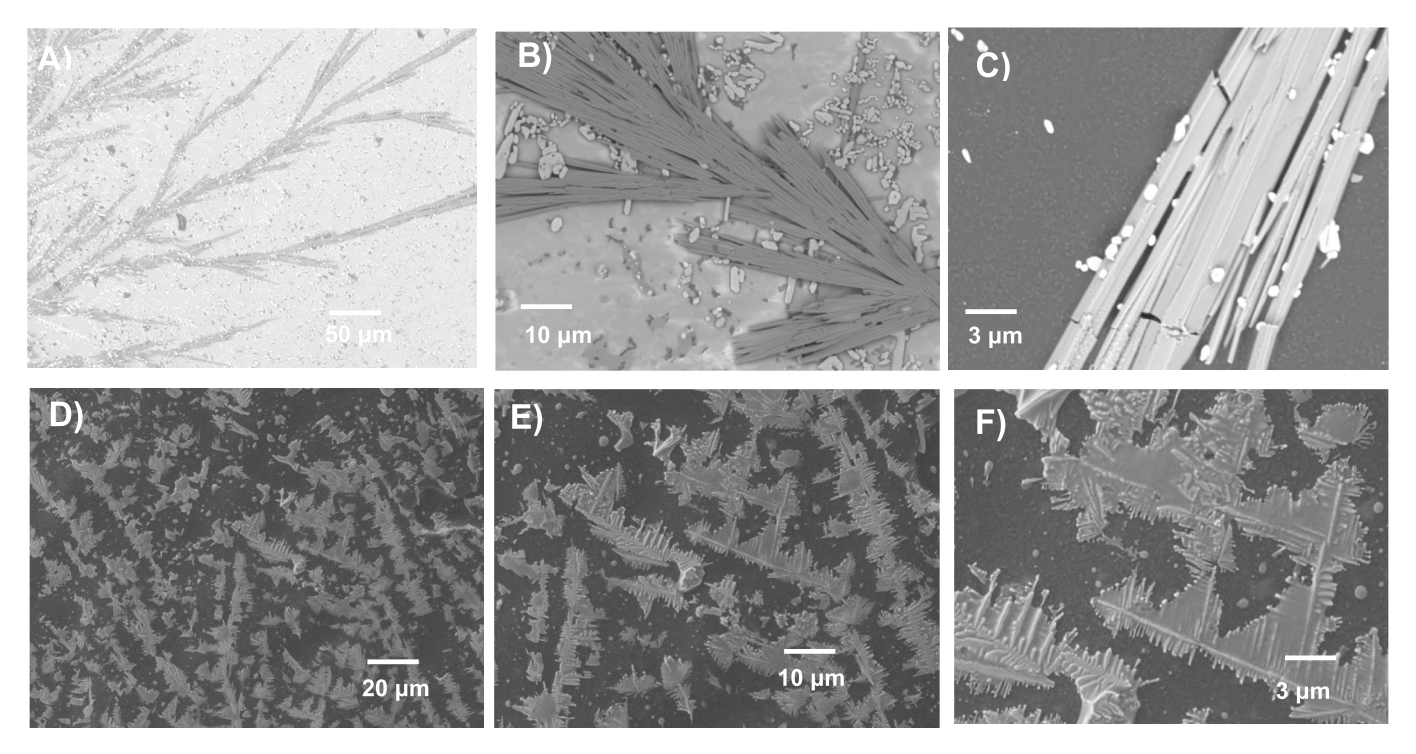


Fig. 8. SEM micrographs of fibrils formed by ABH4 on glass (A) and mica (D) after vortexing 2 min and incubated at 37 °C for 240 min. Panels (B) and (C) show fibril production on glass at different amplifications, and (E) and (F) show fibril production on mica at different amplifications.

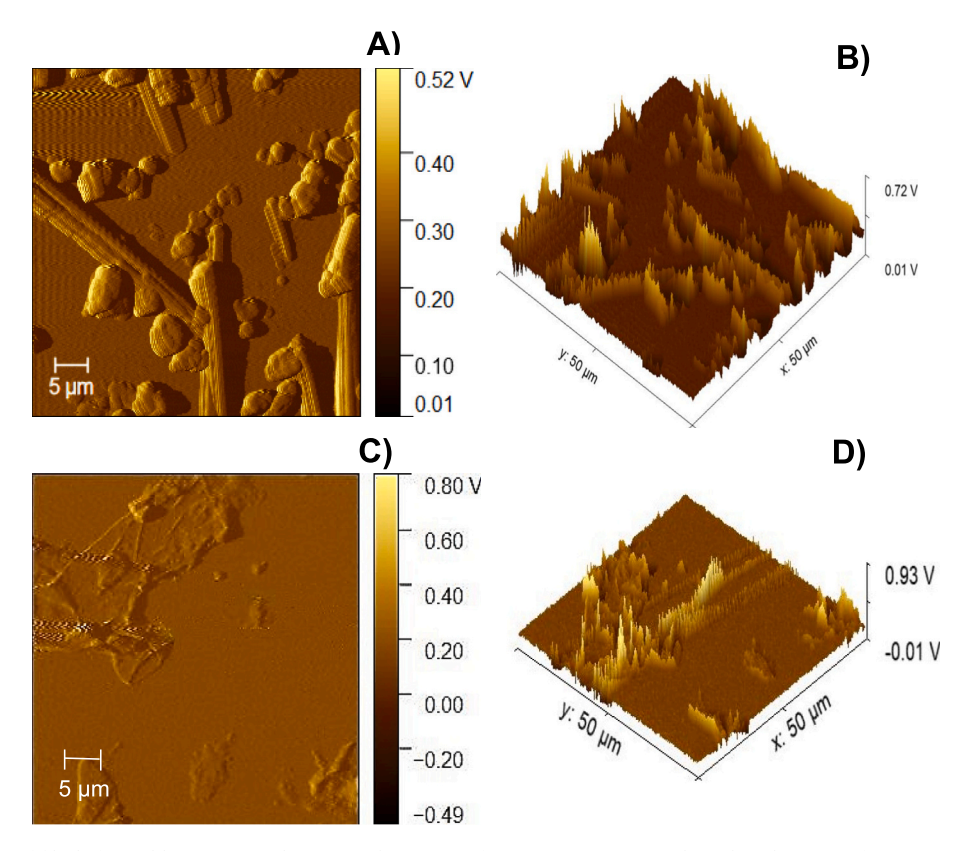


Fig. 9. AFM micrographs of fibrils formed by ABH4 on glass (A) and mica (C) after vortexing 2 min and incubated at 37 °C for 240 min. Panels (B) and (D) show micrographs of fibrils 3D on glass and mica, respectively.

they found isolated fibrils together with oligomers, and Pac3 produced fibrils for both surfaces [36]. ABH4 interacted with different surfaces in this study, forming different amyloid-like structures. However, this

could suggest that ABH4 recognizes glass as a more hydrophobic surface compared to mica; the surfaces presented the following contact angle: glass (16.90 \pm 1.24) and mica (12.72 \pm 1.47), which would imply the

formation of different polymorphs of fibrils.

In this regard, Siddiquee et al. reported that the recombinant hydrophobins class I (EAS $_{\Delta15}$ and DewY) from *Neurospora crassa* produced different structures due to the substrate surface properties can influence the physiochemical properties and the molecular structures of the hydrophobins [37]. By this, the monomers of hydrophobin SC3 diffuse in a water-air interface, where they initially reach the α -helix structure, while at this interface, the α -helix structure changes to the β -sheet state [8].

4. Conclusion

ABH4 from the pinhead of *A. bisporus* showed a molecular weight of 12 kDa, and the protein was able to modify hydrophilic and hydrophobic surfaces. Fibril formation by ABH4 is affected by the nature of the surface, resulting in conformational changes of the protein depending on the assembly surface, producing more crystalline or amorphous structures.

CRediT authorship contribution statement

Jesús Rojas-Osnaya: Writing – review & editing, Writing – original draft, Visualization, Validation, Software, Methodology, Investigation, Formal analysis, Data curation, Conceptualization. Hugo Nájera: Writing – review & editing, Writing – original draft, Visualization, Validation, Supervision, Software, Resources, Project administration, Methodology, Investigation, Funding acquisition, Formal analysis, Data curation, Conceptualization.

Declaration of competing interest

The authors declare that they have no known competing financial interests or personal relationships that could have appeared to influence the work reported in this paper.

Data availability

No data was used for the research described in the article.

Acknowledgments

The authors thank to Consejo Nacional de Humanidades Ciencias y Tecnologías (Conahcyt) for funding and scholarship grant (JRO).

References

- [1] T.B. Ng, Peptides and proteins from fungi, Peptides 25 (2004) 1055-1073.
- [2] X. Xu, H. Yan, J. Chen, X. Zhang, Bioactive proteins from mushrooms, Biotechnol. Adv. 29 (2011) 667–674.
- [3] W.T. Ismaya, R.R. Tjandrawinata, H. Rachmawati, Lectins from the edible mushroom Agaricus bisporus and their therapeutic potentials, Molecules 25 (2020).
- [4] S. Kulkarni, S. Nene, K. Joshi, Production of Hydrophobins from fungi, Process Biochem. 61 (2017) 1–11.
- [5] S.S. Kulkarni, S.N. Nene, K.S. Joshi, Identification and characterization of a hydrophobin Vmh3 from *Pleurotus ostreatus*, Protein Expr. Purif. 195-196 (2022) 106095.
- [6] J.R. Whiteford, P.D. Spanu, Hydrophobins and the interactions between fungi and plants, Mol. Plant Pathol. 3 (2002) 391–400.
- [7] J.M. Kallio, M.B. Linder, J. Rouvinen, Crystal structures of Hydrophobin HFBII in the presence of detergent implicate the formation of fibrils and monolayer films, J. Biol. Chem. 282 (2007) 28733–28739.
- [8] J. Rojas-Osnaya, M. Quintana-Quirino, A. Espinosa-Valencia, A.L. Bravo, H. Nájera, Hydrophobins: multitask proteins, Front. Phys. 12 (2024).
- [9] H.A.B. Wösten, Hydrophobins: multipurpose proteins, Ann. Rev. Microbiol. 55 (2001) 625–646.
- [10] H.A.B. Wösten, M.L. de Vocht, Hydrophobins, the fungal coat unravelled, Biochimica et Biophysica Acta (BBA) - reviews on Biomembranes, 1469 (2000) 70, 96

- [11] H.A.B. Wösten, K. Scholtmeijer, Applications of hydrophobins: current state and perspectives, Appl. Microbiol. Biotechnol. 99 (2015) 1587–1597.
- [12] L.G. Lugones, J.S. Bosscher, K. Scholtmeyer, O.M.H. de Vries, J.G.H. Wessels, An abundant hydrophobin (ABH1) forms hydrophobic rodlet layers in *Agaricus bisporus* fruiting bodies, Microbiology 142 (1996) 1321–1329.
- [13] J.E. Noble, M.J.A. Bailey, Chapter 8 quantitation of protein, in: R.R. Burgess, M. P. Deutscher (Eds.), Methods in Enzymology, Academic Press, Place Published, 2009, pp. 73–95.
- [14] P. Pederson, Protein Methods, 2nd edit., by Daniel M. Bollag, Michael D. Rozycki, and Stuart J. Edelstein. New York: Wiley-Liss, Inc, Proteins: Structure, Function, and Bioinformatics, 28 (1997) 140–140.
- [15] C.A. Schneider, W.S. Rasband, K.W. Eliceiri, NIH image to ImageJ: 25 years of image analysis, Nat. Methods 9 (2012) 671–675.
- [16] A. Esfandiarian, A. Maghsoudian, A. Davarpanah, Y. Tamsilian, S. Kord, Developing a novel procedure in utilizing pendant drop method for determination of ultra-low interfacial tension and surface tension in near-miscibility conditions, J. Pet. Sci. Eng. 215 (2022) 110607.
- [17] C. Pothiratana, W. Fuangsawat, A. Jintapattanakit, C. Teerapatsakul, S. Thachepan, Putative hydrophobins of black poplar mushroom (*Agrocybe cylindracea*), Mycology 12 (2021) 58–67.
- [18] M. Beaulieu, M.B.G. D'Apran, M. Lacroix, Dose rate effect of γ irradiation on phenolic compounds, polyphenol oxidase, and Browning of mushrooms (*Agaricus bisporus*), J. Agric. Food Chem. 47 (1999) 2537–2543.
- [19] C.R. Perry, S.E. Matcham, D.A. Wood, C.F. Thurston, The structure of laccase protein and its synthesis by the commercial mushroom *Agaricus bisporus*, Microbiology 139 (1993) 171–178.
- [20] A.M. Othman, M.A. Elsayed, A.M. Elshafei, M.M. Hassan, Purification and biochemical characterization of two isolated laccase isoforms from Agaricus bisporus CU13 and their potency in dye decolorization, Int. J. Biol. Macromol. 113 (2018) 1142–1148.
- [21] J. Wu, J. Gao, H. Chen, X. Liu, W. Cheng, X. Ma, P. Tong, Purification and characterization of polyphenol oxidase from Agaricus bisporus, Int. J. Food Prop. 16 (2013) 1483–1493.
- [22] C.M. Rafeeq, A.B. Vaishnav, P.P. Manzur Ali, Characterisation and comparative analysis of hydrophobin isolated from Pleurotus floridanus (PfH), Protein Expr. Purif. 182 (2021) 105834.
- [23] Z. Shokribousjein, S.M. Deckers, K. Gebruers, Y. Lorgouilloux, G. Baggerman, H. Verachtert, J.A. Delcour, P. Etienne, J.-M. Rock, C. Michiels, G. Derdelinckx, Hydrophobins, beer foaming and gushing, Cerevisia 35 (2011) 85–101.
- [24] L.G. Lugones, H.A.B. Wös, J.G.H. Wessels, A hydrophobin (ABH3) specifically secreted by vegetatively growing hyphae of *Agaricus bisporus* (common white button mushroom), Microbiology 144 (1998) 2345–2353.
- [25] L.C. Paslay, L. Falgout, D.A. Savin, S. Heinhorst, G.C. Cannon, S.E. Morgan, Kinetics and control of self-assembly of ABH1 Hydrophobin from the edible white button mushroom, Biomacromolecules 14 (2013) 2283–2293.
- [26] I. Macindoe, A.H. Kwan, Q. Ren, V.K. Morris, W. Yang, J.P. Mackay, M. Sunde, Self-assembly of functional, amphipathic amyloid monolayers by the fungal hydrophobin EAS, Proc. Natl. Acad. Sci. USA 109 (2012) E804–E811.
- [27] K.A. Littlejohn, P. Hooley, P.W. Cox, Bioinformatics predicts diverse aspergillus hydrophobins with novel properties, Food Hydrocoll. 27 (2012) 503–516.
- [28] Ł.P. Tymiński, Z. Znajewska, G.B. Dąbrowska, Characteristics and functions of hydrophobins and their use in manifold industries, advancements of, Microbiology 57 (2018) 374–384.
- [29] G. Vigueras, K. Shirai, M. Hernández-Guerrero, M. Morales, S. Revah, Growth of the fungus Paecilomyces lilacinus with n-hexadecane in submerged and solid-state cultures and recovery of hydrophobin proteins, Process Biochem. 49 (2014) 1606–1611.
- [30] H.A. Wösten, F.H. Schuren, J.G. Wessels, Interfacial self-assembly of a hydrophobin into an amphipathic protein membrane mediates fungal attachment to hydrophobic surfaces, EMBO J. 13 (1994), 5848-5854-5854.
- [31] M. Biancalana, S. Koide, Molecular mechanism of Thioflavin-T binding to amyloid fibrils, Biochimica et Biophysica Acta (BBA) - Proteins and Proteomics 1804 (2010) 1405–1412.
- [32] R. Sabaté, I. Lascu, S.J. Saupe, On the binding of Thioflavin-T to HET-s amyloid fibrils assembled at pH 2, J. Struct. Biol. 162 (2008) 387–396.
- [33] M. Torkkeli, R. Serimaa, O. Ikkala, M. Linder, Aggregation and self-assembly of Hydrophobins from *Trichoderma reesei*: low-resolution structural models, Biophys. J. 83 (2002) 2240–2247.
- [34] P. Manavalan, W.C. Johnson, Sensitivity of circular dichroism to protein tertiary structure class, Nature 305 (1983) 831–832.
- [35] V. György, S. Zsolt, Artificial and natural membranes, in: L.F. Christopher (Ed.), Atomic Force Microscopy Investigations into Biology, IntechOpen, 2012. Place Published. Ch. 10.
- [36] P. Cicatiello, P. Dardano, M. Pirozzi, A.M. Gravagnuolo, L. De Stefano, P. Giardina, Self-assembly of two hydrophobins from marine fungi affected by interaction with surfaces, Biotechnol. Bioeng. 114 (2017) 2173–2186.
- [37] R. Siddiquee, V. Lo, C.L. Johnston, A.W. Buffier, S.R. Ball, J.L. Ciofani, Y.C. Zeng, M. Mahjoub, W. Chrzanowski, S. Rezvani-Baboli, L. Brown, C.L.L. Pham, M. Sunde, A.H. Kwan, Surface-induced Hydrophobin assemblies with versatile properties and distinct underlying structures, Biomacromolecules 24 (2023) 4783–4797.